

Cyclooligomerization of a Helix-Bearing Template into Macrocycles Bearing Multiple Helices

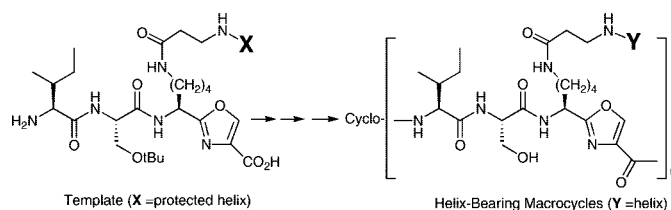
Renée L. Beyer, Yogendra Singh, and David P. Fairlie*

Centre for Drug Design and Development, Institute for Molecular Bioscience,
University of Queensland, Brisbane QLD 4072, Australia

d.fairlie@imb.uq.edu.au

Received June 3, 2008

ABSTRACT



Cyclooligomerization was investigated for separating and spatially arranging helical peptides as discontinuous surfaces. Tetrapeptide H-[Ile-Ser-Lys(Ox)]-OH, containing a turn-inducing oxazole constraint, was connected through its lysine side chain via a β -alanine linker to the C-terminus of a two-turn helical nonapeptide Ac-(cyclo-4,8)-LRL [KARAD](Aib). The resulting helix-appended template was self-condensed and cyclized to a library of macrocycles ($n = 2-6$) containing multiple (2-6) helices. An NMR structure shows retention of α helicity in the cyclotrimer ($n = 3$).

Protein function is frequently mediated by structural motifs (e.g., helices, turns, strands/sheets) well separated in sequence but brought close together by polypeptide folding. Such “discontinuous” peptide surfaces have been extremely difficult to recreate in small molecules because of the thermodynamic instability of short peptide structures outside of protein environments and the lack of conformational control in organizing the three-dimensional location and orientation of structural motifs over large distances.¹ One potentially useful approach to creating large molecules with motifs at specific locations in three-dimensional space is cyclooligo-

merization, in which templates (either multiple copies of one template or multiple templates) are combined and conformationally constrained by cyclization.²⁻⁴ Cyclic peptides are useful scaffolds for supporting bundles of interacting helices⁵ but can also be used to support noninteracting helices as here.

Cyclooligomerization is a valuable entry to large macrocycles and has been used to synthesize marine cyclic peptides and analogues, with metal-binding, cytotoxic, antibacterial, antiviral, and other pharmacological activities as well as cylindrical, conical, and saddle-shaped cavitands.²⁻⁴ Frequently, a turn-inducing constraint (e.g., oxazole (Ox), thiazole (Thz)) is present in the template to encourage

(1) (a) Schneider, J. P.; Kelly, J. W. *Chem. Rev.* **1995**, *95*, 2169. (b) Fairlie, D. P.; West, M. W.; Wong, A. K. *Curr. Med. Chem.* **1998**, *5*, 29. (c) Singh, Y.; Stoermer, M. J.; Lucke, A.; Guthrie, T.; Fairlie, D. P. *J. Am. Chem. Soc.* **2005**, *127*, 6563.

(2) (a) Sokolenko, N.; Abbenante, G.; Scanlon, M. J.; Jones, A.; Gahan, L. R.; Hanson, G. R.; Fairlie, D. P. *J. Am. Chem. Soc.* **1999**, *121*, 2603-4. (b) Singh, Y.; Sokolenko, N.; Kelso, M. J.; Gahan, L. R.; Abbenante, G.; Fairlie, D. P. *J. Am. Chem. Soc.* **2001**, *123*, 333-4. (c) Singh, Y.; Stoermer, M. J.; Lucke, A. J.; Glenn, M. P.; Fairlie, D. P. *Org. Lett.* **2002**, *4*, 3367-3370. (d) Singh, Y.; Hoang, H. N.; Flanagan, B.; Fairlie, D. P. *Org. Lett.* **2006**, *8*, 1053-6. (e) Abbenante, G.; Fairlie, D. P.; Gahan, L. R.; Hanson, G. R.; Pierens, G.; van den Brenk, A. L. *J. Am. Chem. Soc.* **1996**, *118*, 10384.

(3) (a) Wipf, P.; Miller, C. P.; Grant, C. M. *Tetrahedron* **2000**, *56*, 9143-9150. (b) Wipf, P. *Chem. Rev.* **1995**, *95*, 2115.

(4) (a) Somogyi, L.; Haberhauer, G.; Rebek, J. *Tetrahedron* **2001**, *57*, 1699-1708. (b) Bertram, A.; Blake, A. J.; de Turiso, F. G. L.; Hannam, J. S.; Jolliffe, K. A.; Pattenden, G.; Skae, M. *Tetrahedron* **2003**, *59*, 6979-6990.

(5) (a) Tuchscherer, G.; Mutter, M. *J. Biotechnol.* **1995**, *41*, 197-210. (b) Mutter, M.; Hersperger, R.; Gubernator, K.; Müller, K. *Proteins* **1989**, *5*, 13-21. (c) Singh, Y.; Dolphin, G. T.; Razkin, J.; Dumy, P. *ChemBioChem* **2006**, *7*, 1298-1314. (d) Wong, A.; Jacobsen, M. P.; Winzor, D. J.; Fairlie, D. P. *J. Am. Chem. Soc.* **1998**, *120*, 3836-3841.

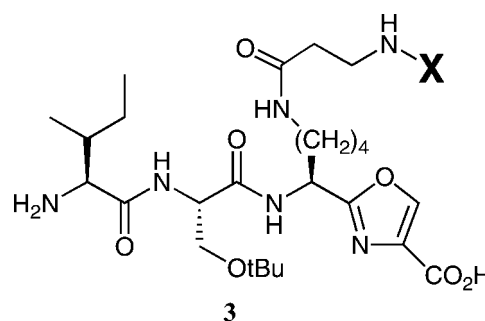
cyclization while template concentration is varied to influence competing rates of chain-extending (oligomerization) versus chain-terminating (cyclization) steps that determine the size distribution of macrocyclic products. For example, the one-pot cyclooligomerization of tetrapeptide H-Ile-Ser-D-Val(Thz)-OH produced a series of constrained macrocycles cyclo-[Ile-Ser-D-Val(Thz)]_n (*n* = 2–19)^{2a} with predominantly dimer formed at 10⁻²–10⁻⁴ M concentrations of tetrapeptide, but at 0.15 M there were up to 19 units assembled in a giant macrocycle with 228 atoms in the ring. A similar template H-[Glu-Ser-Lys(Thz)]-OH, containing a loop formed by linking Glu and Lys side chains through a Val-Ile dipeptide linker, undergoes a one-pot self-assembly to a library of macrocycles containing 2–10 units with 2–10 appended loops.^{2d} Higher oligomers formed at 0.1 M template concentration, while mainly dimer formed at 10⁻³ M.^{2d}

The α helix makes up about one-third of the protein structure, and the positioning of noncommunicating helical elements at separate locations on a large scaffold could potentially enable mimicry of some biologically important protein surfaces.¹ Here, we describe the use of cyclooligomerization to create a library of macrocyclic scaffolds with multiple appended two-turn helical motifs from the helix-bearing template {–Ile-Ser-Lys(Helix)Ox–} containing a turn-inducing oxazole constraint.

The first objective was to constrain a short peptide to adopt a stable helix. Ac-(cyclo-1,5)Ac[KARAD]-NH₂ has been reported to be highly α -helical,⁶ so we chose this with a C-terminal Aib (to avoid racemization) and three N-terminal helix-favoring amino acids (LRL) to create a two-turn helical nonapeptide. The protected nine-residue peptide Ac-(cyclo-4,8)-LR(Pbf)L[KAR(Pbf)AD](Aib)-OH (**1**) was synthesized manually by solid-phase methods using HBTU/DIPEA activation and Fmoc chemistry on trityl chloride-polystyrene resin (Supporting Information). Arginine was orthogonally protected with 2,2,4,6,7-pentamethylidihydrobenzofuran-5-sulfonyl (Pbf), and lysine and aspartic acid side chains were protected with alloc and allyl groups, respectively. Simultaneous removal of alloc and allyl protecting groups from resin-bound fully assembled peptide was accomplished with Pd(PPh₃)₄ in the presence of 1,3-dimethylbarbituric acid in dichloromethane. The exposed side-chain amine and acid were coupled using BOP in DMF-containing DIPEA. Cleavage of peptide from resin with Arg side chains protected using 1% TFA in CH₂Cl₂ gave 51% peptide (**1**). Treatment with TFA in H₂O with triisopropylsilane as scavenger removed Pbf protecting groups to produce the more water-soluble Ac-(cyclo-4,8)-LRL[KARAD](Aib)-OH (**2**).

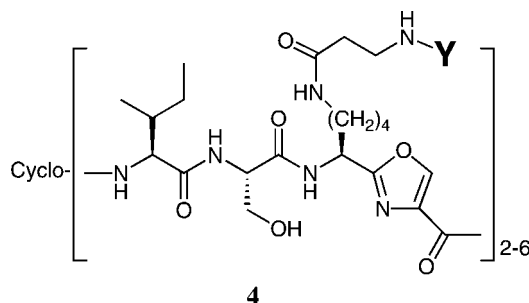
Second, template **3** had to be created with peptide **1** attached via a β -alanine spacer to the Lys side chain in tetrapeptide analogue H-[Ile-Ser-Lys(Ox)]-OH. Boc-Lys(Cbz)-(Ox)-OMe was first converted to Fmoc-Lys(Alloc)(Ox)-OH (Supporting Information), the different protecting groups on Lys being compatible with subsequent steps. Catalytic hydrogenolysis (10% Pd/C) of the Cbz protecting group followed by reacting the free amino group of Boc-Lys-

(H)(Ox)-OMe with allyl chloroformate in the presence of DIPEA, and hydrolysis of the methyl ester with LiOH, gave Boc-Lys(Alloc)(Ox)-OH. Removal of the N-terminal Boc protecting group with TFA and treatment with Fmoc-OSu gave the oxazole Fmoc-Lys(Alloc)(Ox)-OH in 63% overall yield after purification. The amino group of β -alanine was protected using allyl chloroformate before coupling to Fmoc-IleSer(*t*Bu)Lys(Alloc)(Ox)-OH that had been assembled on TCP resin (Supporting Information). Removal of the Alloc protecting group from β -alanine rendered the amine free for coupling with peptide **1** Ac-(cyclo-4,8)-LR(Pbf)L[KAR(Pbf)AD](Aib)-OH using a mixture of BOP, HOAt, and DIPEA in DMF. The N-terminal Fmoc protecting group was removed with 50% piperidine in DMF. The peptide was cleaved from the resin (1% TFA in CH₂Cl₂), retaining side chain protecting groups on Arg and Ser in order to obtain the monomeric unit **3**, H-Ile-Ser(O*t*Bu)-Lys(β Ala-X)(Ox)-OH.



(X = Ac-(cyclo-4,8)-LR(Pbf)L[KAR(Pbf)AD](Aib)-)

Third, cyclooligomerization of **3** was conducted at 0.50 M using coupling agent BOP and base DIPEA in DMF, producing a series of macrocycles cyclo-[**3**]_n where *n* = 2–6. The crude deprotected mixture was analyzed by matrix-assisted laser desorption ionization time-of-flight mass spectrometry (MALDI-TOF) revealing crude deprotected macrocycles, dimer (**4b**) (*m/e* 2999.8), trimer (**4c**) (*m/e* 4499.6), and tetramer (**4d**) (*m/e* 5999.5) in a ratio of 13:4:1, as well as trace amounts of cyclic pentamer (**4e**) (*m/e* 7499.4) and cyclic hexamer (**4f**) (*m/e* 8999.3) as shown in Figure 1. Purification was achieved by reversed-phase HPLC using C18 silica columns.



(Y = Ac-(cyclo-4,8)-LRL[KARAD](Aib)-).

The macrocyclic dimer (**4b**) and trimer (**4c**) were isolated and characterized by electrospray mass spectrometry (ESMS) and MALDI-TOF. ESMS spectra (Figure 2) show *m/z* peaks

(6) Shepherd, N. E.; Hoang, H. N.; Abbenante, G.; Fairlie, D. P. *J. Am. Chem. Soc.* **2005**, *127*, 2974–2983.

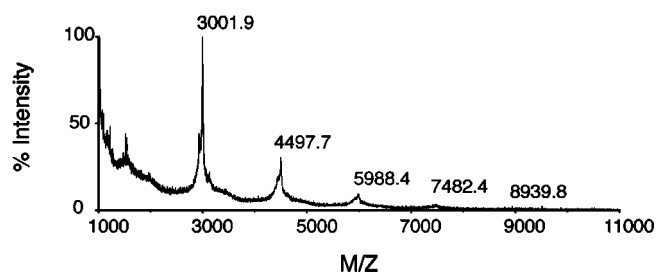


Figure 1. MALDI-TOF spectrum of crude deprotected mixture of macrocycles **4b–f** from cyclooligomerization of 0.5 **M 3**. Magnified spectra for purified macrocycles and mixtures are shown in the Supporting Information.

for cyclic dimer (**4b**) at $750.45 (M + 4H^+)/4$ and $1002.29 (M + 3H^+)/3$, while cyclic trimer (**4c**) has peaks at $750.70 (M + 6H^+)/6$, $900.93 (M + 5H^+)/5$, and $1125.42 (M + 4H^+)/4$. Reconstructed molecular ions confirmed product stoichiometry with peaks in isotopic distributions separated by 1 amu. Isotope patterns for both products were as expected for the molecular ion. MALDI-TOF mass spectra were obtained for isolated cyclic dimer (**4b**) and trimer (**4c**) and for mixtures of cyclic tetramer (**4d**), pentamer (**4e**), and hexamer (**4f**) (Supporting Information).

Circular dichroism spectra are shown for nonapeptide **2** and cyclic trimer **4c** at 5 °C (Figure 3), indicating appreciable α -helicity although it is difficult to quantify using equations developed for polypeptides. The mean residue ellipticity ratio $[\theta]_{222}/[\theta]_{208}$ for **2** was 0.74 at 5 °C (0.58 at 25 °C) and for **4c** it was 0.84 at 5 °C (0.81 at 25 °C), which is in the range expected for an α -helix ($\sim 0.7–1.1$).⁷ The slight increase in helicity on the template may reflect a H-bond interaction between template and C-terminus of peptide **2**.

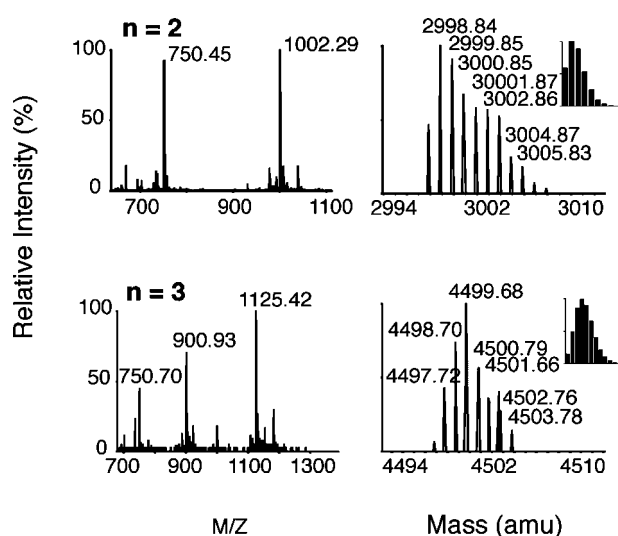


Figure 2. Left: Electrospray mass spectra for deprotected cyclic dimer (**4b**) and trimer (**4c**). Right: Reconstructed molecular ion showing isotope distribution vs (inset) calculated isotopic distribution which match, thereby confirming compositions.

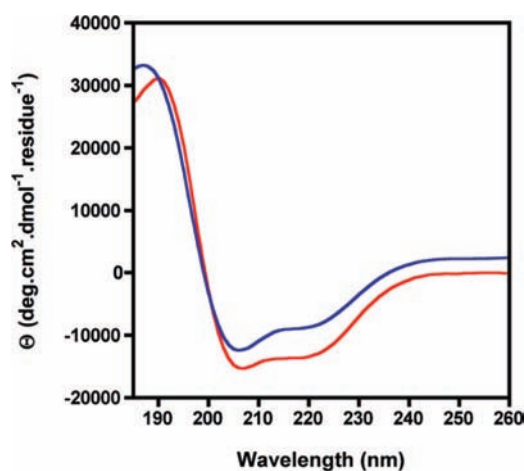


Figure 3. Circular dichroism spectra for 60 μM Ac-(cyclo-4,8)-LRL[KARAD](Aib)-OH (**2**, blue line) versus deprotected 50 μM cyclic trimer (**4c**, red line) in 10 mM phosphate buffer pH 7 at 5 °C.

Proton NMR spectra recorded in $\text{H}_2\text{O}/\text{D}_2\text{O}$ (9:1) for **2** and **4c** at 5 and 25 °C show features characteristic of α -helicity. For **2**, several $^3J_{\text{NHCH}\alpha}$ coupling constants are < 6 Hz (3 at 25 °C, 5 at 5 °C). α helicity is often indicated when three or more consecutive residues display $^3J_{\text{NHCH}\alpha} < 6$ Hz,⁸ and this is seen for Lys3-Ala5 at 5 °C. The data at 25 °C are consistent with some contributions from random or 3_{10} helical structures. For cyclic trimer **4c**, there was amide-NH signal overlap at 298 and 288 K; at 278 K, the amide NH resonances were sufficiently dispersed to allow assignment but too broad to obtain coupling constants. A dqf-COSYwg spectrum enabled four coupling constants to be determined, two being < 6 Hz.

The magnitude of the amide NH shift with temperature is an indicator of the degree to which an amide NH proton is protected from solvation.⁹ H-bonded amide protons for peptides in water usually have low temperature coefficients ($\Delta\delta/T \leq 5$ ppb/K).¹⁰ For peptide **2** within trimer **4c**, an α -helical structure would have NH \cdots OC hydrogen bonds from Lys4 to Aib9. This was observed for Leu3-Ala5, -Ala7, and -Aib9 with Arg6 and Asp8 displaying $\Delta\delta/T \sim 5$ ppb/K (Supporting Information, Figure S10). Surprisingly, a low temperature coefficient was observed for Leu3 which could be involved in an NH \cdots OC (i) to ($i + 3$) hydrogen bond with the N-terminal acetyl, typical¹⁰ of a 3_{10} -helical turn terminating an α helix.

2D-NMR spectra for **4c** provided NOE data (Supporting Information) consistent with α -helicity, with short $d_{\alpha\text{N}}(i, i$

(7) Woody, R. W. In *Circular Dichroism and the Conformational Analysis of Biomolecules*; Fasman, G. D., Ed.; Plenum Press: New York, 1996; pp 25–67.

(8) (a) Pardi, A.; Billeter, M.; Wuthrich, K. *J. Mol. Biol.* **1984**, *180*, 741–751. (b) Dyson, H. J.; Wright, P. E. *Annu. Rev. Biophys. Biophys. Chem.* **1991**, *20*, 519–538.

(9) (a) Kessler, H. *Angew. Chem., Int. Ed.* **1982**, *21*, 512–523. (b) Dyson, H. J.; Cross, K. J.; Houghten, R. A.; Wilson, I. A.; Wright, P. E.; Lerner, R. A. *Nature* **1985**, *318*, 480–483.

(10) Barlow, D. J.; Thornton, J. M. *J. Mol. Biol.* **1988**, *201*, 601–619.

+ 1), $d_{\text{NN}}(i, i + 1)$, $d_{\alpha\text{N}}(i, i + 3)$, $d_{\alpha\text{N}}(i, i + 4)$, and $d_{\alpha\beta}(i, i + 3)$ distances.¹¹ The proportion of $d_{\alpha\text{N}}(i, i + 4)$ and $d_{\alpha\text{N}}(i, i + 2)$ NOEs indicated α -helicity rather than 3_{10} -helicity for the nonapeptide in **4c**, although some 3_{10} -helicity is evident at the N-terminus. The structure for the nonapeptide portion of deprotected cyclic trimer **4c** in H₂O/D₂O (9:1) at 278 K was determined from 98 NOE distance restraints (44 intrasidue, 36 sequential, 18 medium range $i \rightarrow i + 2$, $i \rightarrow i + 3$, and $i \rightarrow i + 4$) and eight backbone ϕ -dihedral angle restraints, two of which were derived from the dqf-COSYwg spectrum. The structures were calculated in XPLOR using a dynamic simulated annealing protocol in a geometric force field and were energy minimized using a modified CHARMM force field. No hydrogen bond constraints were included in the final structures (Figure 4). The structure may have been

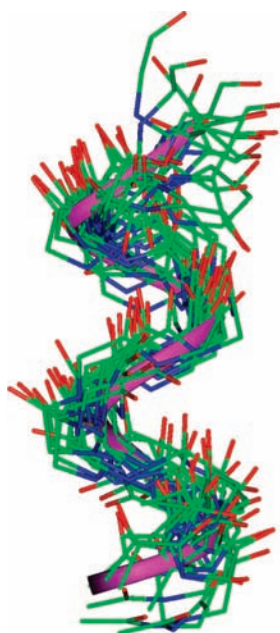


Figure 4. Backbone superimposition of 20 lowest energy structures for nonapeptide component Ac-(cyclo-4,8)-LRL[KARAD](Aib)- of cyclic trimer **4c** (ave backbone pairwise rmsd = 1.72 Å) in H₂O/D₂O (9:1). Amide protons omitted for clarity and pink ribbon is the lowest energy structure (an α -helix).

more accurate if it had been possible to determine all backbone dihedral angles ϕ from $^3J_{\text{NHCH}\alpha}$ coupling constants. Instead, structures were compared with those calculated using

(11) Wüthrich, K.; Billeter, M.; Braun, W. *J. Mol. Biol.* **1984**, *180*, 715–740.

the four CO (i) to NH ($i + 4$) hydrogen bonds suggested by VT NMR data and with those calculated using the hydrogen bonds and the six additional dihedral angle restraints $\phi = -100 \pm 80^\circ$. The nonapeptide in **4c** is α -helical (Figure 4), and thus, CD and NMR data show that structural integrity of peptide **2** is maintained during cyclooligomerization of **3**.

Cyclooligomerization of a tetrapeptide, containing an oxazole turn-inducing constraint and an appended helical peptide, has provided a one-pot entry to macrocycles of different sizes with multiple numbers of appended α -helices. The product distribution of macrocycles **4b–f** ($n = 2–6$) was less extensive than previously observed for similar tetrapeptide templates without appendages ($n = 2–19$)^{2a} or with appended loops ($n = 2–10$),^{2d} which may reflect steric hindrance from the appended helical peptide protected with bulky Pbf groups. Nevertheless, the distribution contrasts with other reported cyclooligomerizations of peptide–heterocycle constructs for which mainly cyclic dimer was obtained albeit at low concentrations (2–50 mM).^{3,4} In this report, the helical nonapeptide **2** was successfully piggybacked on the template through multiple tandem polymerization and cyclization reactions without loss of its structural integrity. Lack of intramolecular NOEs between helices attached to the macrocycles and the sizes of the macrocycles themselves ($n \geq 3$) together suggest that the appended helices are likely radially separated and organized in different three-dimensional spaces. This could be of value in mimicking some noncommunicating discontinuous surfaces of proteins, where approaches have previously been limited to bundling adjacent peptides together for interaction and stabilization of α -helicity.⁵ Helices in cyclic hexamer **4f** are measured to be 26 Å apart, assuming the macrocycle is pseudoplanar like close counterparts.² The control in these macrocycles over distance and spatial orientation of the helices is a positive step toward mimicking discontinuous protein surfaces. Although examples here are macrocycles with multiple copies of a single helical motif, this approach lends itself to producing macrocycles from different templates² and with different appended structural motifs.^{2d}

Acknowledgment. We thank the ARC for financial support and for a Federation Fellowship to D.P.F.

Supporting Information Available: Detailed syntheses and compound characterization including NMR spectra, mass spectra, HPLC retention times, 15 figures, 7 schemes, and 1 table. This material is available free of charge via the Internet at <http://pubs.acs.org>.

OL801040C